Room Temperature Crystal Structure of $La_{1/3}Zr_2(PO_4)_3$, a NASICON-type Compound

M. Barre,*[,†,‡] M. P. Crosnier-Lopez,[†,‡] F. Le Berre,[†,‡] J. Emery,[‡,§] E. Suard,[||] and J.-L. Fourquet[†,‡]

Laboratoire des Oxydes et Fluorures (UMR CNRS 6010), Laboratoire de Physique de l'Etat Condensé (UMR CNRS 6087), and Institut de Recherche en Ingéniérie Moléculaire et Matériaux Fonctionnels (FR CNRS 2575), Faculté des Sciences et Techniques, Université du Maine, Av. O. Messiaen, 72085 Le Mans Cedex 9, France, and Institut Laüe-Langevin, 6 rue G. Horowitz, 38042 Grenoble Cedex 9, France

Received July 12, 2005. Revised Manuscript Received October 14, 2005

The room-temperature crystal structure of $La_{1/3}Zr_2(PO_4)_3$, synthesized by the Pechini sol−gel process, has been determined from X-ray powder and neutron diffraction data [space group $P\bar{3}$, $Z = 6$, $a = 8.7378(2)$ Å, $c = 23.2156(7)$ Å]. It derives from the NASICON-structural type (space group $R\bar{3}c$); if the $[Zr_2(PO_4)_3]^-$ network is preserved, the two La^{3+} ions are found quasiordered along the *c* axis: 1 on the 1a (0, 0, 0), 0.82 on the 1b (0, 0, $^1/_2$) sites, and the remaining 0.18 La^{3+} ions occupying partially a 2d site ($^1/_3$, $^2/_3$, 0.667(5)). One and two dimensional ^{31}P nuclear magnetic resonance (1D and 2D, respectively) investigations confirm this distribution.

Introduction

Since the work in 1967 of Sljukic et al.[1] on $NaZr_2(PO_4)_3$, many related zirconium phosphates have been extensively studied. The crystal structure of the sodium phase was determined in 1968 by Hagman and Kierkegaard[2] but its Na^+ ionic conductivity was only recognized by Goodenough et al. in 1976.[3] Among the large amount of substituted $M_xZr_2(PO_4)_3$ NASICON phosphates, the $RE_{1/3}Zr_2(PO_4)_3$ family was first pointed out and synthesized in 1994 by Alami Talbi et al.[4] but the crystal structures of these compounds remained unknown till now. Very recently, some of these materials were found to be trivalent cationic solid electrolytes[5−11] and described as potential hosts for actinide immobilization.[12] So, we decided to determine some of their crystal structures; this present paper deals with the description of that of the $La_{1/3}Zr_2(PO_4)_3$ compound.

Experimental Section

Synthesis. $La_{1/3}Zr_2(PO_4)_3$ powder was synthesized by the Pechini method[13] from La_2O_3, $ZrOCl_2{\cdot}8H_2O$ and $NH_4H_2PO_4$ in stoichiometric ratios. The procedure is shown in Figure 1. After dissolving La_2O_3 in diluted nitric acid (∼2 N) and $ZrOCl_2{\cdot}8H_2O$ in deionized water, the two solutions were mixed together and the desired amount of citric acid (CA) (molar ratio CA/M: 15/1; M = [La] + [Zr]) was added. After homogenization of the solution containing cations, $NH_4H_2PO_4$ dissolved in water and ethylene glycol (EG) (molar ratio CA/EG: 1/4) were added. Esterification between CA and EG was accelerated by heating at 100 °C to produce a viscous gel that was dried at 150 °C. This gel was then heated at 350 °C in air to obtain a black solid that was ground into powder called "the precursor". A first heat treatment was performed in a furnace between 800 and 1000 °C before a final annealing at 1100 °C for 2 h, which produced a single phase and well-crystallized $La_{1/3}Zr_2(PO_4)_3$ white powder. With increasing heating temperature and time, more complete crystallization is obtained, but some impurity phases ZrP_2O_7 and $Zr_2O(PO_4)_3$ appear.

Structural Characterization. The X-ray and neutron powder diffraction patterns were recorded in air with Cu Kα radiation on a PANalytical X'pert Pro diffractometer equipped with the X'celerator detector and on ILL D2B high-resolution neutron diffractometer. The details of data collections are presented in Table 1. Structure refinement was carried out by the Rietveld method, using Fullprof profile refinement program.[14]

NMR Measurements. The room temperature ^{31}P NMR spectra were recorded on powdered samples with a Bruker Avance (DSX)

* Corresponding author. Phone: 33 2 43 83 26 24. Fax: 33 2 43 83 35 06. E-mail: maud.barre.etu@univ-lemans.fr.
† Laboratoire des Oxydes et Fluorures, Université du Maine.
‡ Institut de Recherche en Ingéniérie Moléculaire et Matériaux Fonctionnels, Université du Maine.
§ Laboratoire de Physique de l'Etat Condensé, Université du Maine.
|| Institut Laüe-Langevin.

(1) Sljukic, M.; Matkovic, B.; Prodic, B.; Scavnicar, S. *Croatia Chem. Acta*. **1967**, *39*, 145.
(2) Hagman, L. O.; Kierkegaard, P. *Acta Chem. Scand*. **1968**, *2*, 1822.
(3) Goodenough, J. B.; Hong, H. Y.-P.; Kafalas, J. A. *Mater. Res. Bull*. **1976**, *1*, 203.
(4) Alami Talbi, M.; Brochu, R.; Parent, C.; Rabardel, L.; Le Flem, G. *J. Solid State Chem*. **1994**, *110*, 350.
(5) Tamura, S.; Imanaka, N.; Adachi, G. *Solid State Ionics*. **2000**, *136−137*, 423.
(6) Tamura, S.; Imanaka, N.; Adachi, G. *J. Mater. Sci. Lett*. **2001**, *20*, 2123.
(7) Tamura, S.; Imanaka, N.; Kamikawa, M.; Adachi, G. *Sensors Actuators*. **2001**, *B 73*, 205.
(8) Tamura, S.; Imanaka, N.; Adachi, G. *J. Alloys Compd*. **2001**, *323−324*, 540.
(9) Imanaka, N.; Adachi, G.-Y. *J. Alloys Compd*. **2002**, *344*, 137.
(10) Tamura, S.; Imanaka, N.; Adachi, G. *Solid State Ionics* **2002**, *154−155*, 767.
(11) Tamura, S.; Imanaka, N.; Adachi, G. *Recent Res. Dev. Solid State Ionics* **2003**, *1*, 189.
(12) Bois, L.; Guittet, M. J.; Carrot, F.; Trocellier, P.; Gauthier-Soyer, M. *J. Nucl. Mater*. **2001**, *297*, *129*.
(13) (a) Pechini, M. P. U.S. Patent 3,330,697, 1967. (b) Kakihana, M. *J. Sol-Gel Sci. Technol*. **1996**, *6*, *7*.
(14) Rodriguez-Carvajal, J. *FULLPROF.2K*, Version 3.20; Institut Laüe-Langevin, Grenoble, 2005.

10.1021/cm0515045 CCC: $30.25
Published on Web 11/18/2005

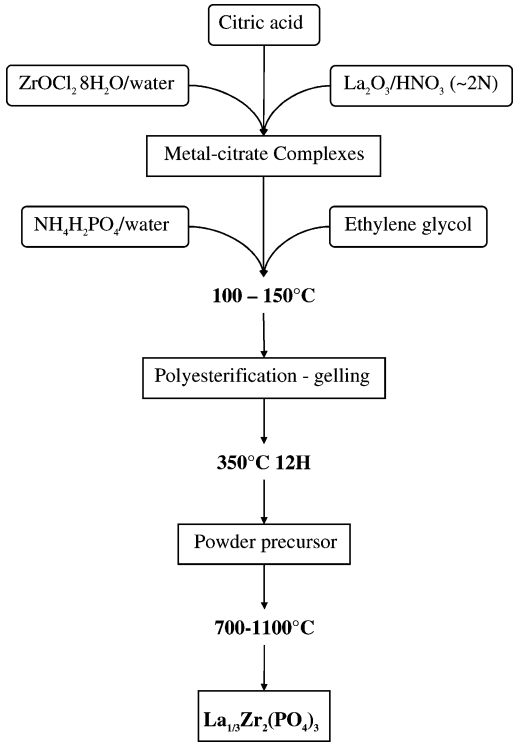

Figure 1. Flowchart for the preparation of $La_{1/3}Zr_2(PO_4)_3$ powder by the Pechini method.

Table 1. Conditions of X-ray and Neutron Data Collection for $La_{1/3}Zr_2(PO_4)_3$

diffractometer	Philips X'pert PRO	D2B (ILL)
radiation	X-ray Cu Kα	neutron 1.59491(1) Å
angular range (deg 2θ)	5.00−129.99	0.1−140
step scan increment (deg 2θ)	0.017	0.05
counting time	150 s step^{-1}	4 h
temperature (K)	298	298

Table 2. NMR Experimental Conditions

parameters	1D	2D
pulse length (μs)	3.57	3.57
dead time (μs)	10	10
recycle time (s)	1000	40
resonance frequency	121.443	121.443
MAS spinning speed (kHz)	10	10
number of scan	8	16
number of digitized points	1024	256 × 196
referencing 0 ppm	H_3PO_4 (85%)	H_3PO_4 (85%)

300 spectrometer, working at $\nu_0 = 121.44$ MHz and using a 4 mm MAS probe spinning up to 15 kHz. The amplitude of the radio frequency field for ^{31}P is $\nu_1 = 70$ kHz. In a first step, magic angle spinning (MAS) (1D) one-pulse experiments were performed on ^{31}P. The experimental parameters are reported in Table 2. DMFIT software[15] is used to fit the spectra and obtain the line widths, the peaks positions, and the percentage of each contribution.

2D Experiments: Connectivity between ^{31}P Nuclei. To characterize connectivity between P atoms, we have performed double quantum experiments (DQ). Increased resolution and sensitivity require MAS in solids in order to suppress the chemical shift anisotropy, but unfortunately MAS also suppresses the dipolar coupling.

Dipolar recovery methods reintroduce the dipolar coupling in the presence of MAS. Several methods were proposed.[16−21] C7[20] and POSTC7[21] are the most efficient with respect to all forms of chemical shifts and radio frequency amplitude errors. POSTC7 is used in our experiments. This sequence involves rotor-synchronized radio frequency pulse cycles combined in a 7-fold symmetric phase shifted scheme. The experimental strategy for DQ experiments[22] is based on two-dimensional experiments: Preparation, excitation of the DQ (C7), evolution of the DQ during t_1 (mixing), reconversion (POSTC7), and detection in t_2.

An appropriate phase cycling selects the DQ coherence and the purely absorption 2D experiment is achieved by using the STATES method.[23]

Since the ^{31}P is a $I = {}^1/_2$ spin nucleus, DQ needs two coupled spins; so in a DQ experiment only coupled spins appear in the 2D diagram, and the peaks in the (Ω_1, Ω_2) plane result from dipolar coupled spins: along the diagonal the peaks account for coupled nuclei with the same chemical shift, when the peaks out of the diagonal account for coupled nuclei with different chemical shifts.

Results and Discussion

XRD Study. In contrast to $La_{1/3}Ti_2(PO_4)_3$, belonging to the rhombohedral $R\bar{3}$ space group,[24] the XRD pattern of the title compound is readily indexed with a primitive hexagonal unit cell, the parameters of which [$a = 8.7492(2)$ Å and $c = 23.2483(5)$ Å] are close to those of other NASICON-type compounds and in very good agreement with those proposed by Alami Talbi et al.[4] It is clear that the rhombohedral space groups $R\bar{3}$ and $R\bar{3}c$—usually encountered for many NASICON type phases—are excluded here due to the presence of the (002) and (004) diffraction peaks on the X-ray powder diffraction pattern (Cu Kα) at respectively the 2θ values 7.60° and 15.25° (Figure 2). The similarity between the parameters of the unit cell with those of other NASICON-type phases is strongly in favor of the preservation of the $[Zr_2(PO_4)_3]^-$ typical network in the title compound and suggests that it belongs to the trigonal crystal system by lowering of the symmetry. So, owing to the results of the pattern-matching calculations (Fullprof[14]) leading to the absence of reflection conditions, and excluding first the corresponding seven primitive hexagonal space groups belonging to the 6/*m* and 6/*mmm* Laüe classes, the remaining possible trigonal space groups are $P\bar{3}1m$, $P31m$, $P312$ (subgroups of $P6/mmm$), $P\bar{3}m1$, $P3m1$, $P321$ (subgroups of $R\bar{3}m$), $P\bar{3}$, and $P3$ (subgroups of $R\bar{3}$). So, we start the Rietveld calculations in the $P\bar{3}$ space group with an atomic model strictly transposed from that classically described in

(15) Massiot, D.; Fayon, F.; Capron, M.; King, I.; Le Calvé, S.; Alonso, B.; Durand, J.-O.; Bujoli, B.; Gan, Z.; Hoaston, G. *Magn. Reson. Chem.* **2002**, *40*, 70.

(16) Tycko, R.; Dabbagh G. *J. Chem. Phys. Lett.* **1990**, *173*, 461.
(17) Tycko, R.; Dabbagh, G. *J. Am. Chem. Soc.* **1991**, *113*, 9444.
(18) Nielsen, N. C.; Bildsoe, H.; Jakobsen, H. J.; Levitt, M. H. *J. Chem. Phys.* **1994**, *101*, 1805.
(19) Sun, B. Q.; Costa, P. R.; Koscisko, D.; Lansbury, P. T.; Griffin, R. G. *J. Chem. Phys.* **1995**, *102*, 702.
(20) Lur, Y. K.; Kurur, N. D.; Helmle, M.; Johannessen, O.; Nielsen, N. C.; Levitt, M. H. *Chem. Phys. Lett.* **1995**, *242*, 304.
(21) Hohwy, M.; Jakobsen, H. J.; Eden, M.; Levitt, M. H.; Nielsen, N. C. *J. Chem. Phys.* **1998**, *108*, 2686.
(22) Ernst, R. R.; Bodenhausen, G.; Wokaun, A. *Principles of Nuclear Magnetic Resonance in One and Two Dimensions*; Clarendon Press: Oxford, 1987.
(23) States, D. J.; Haberkorn, R. A.; Ruben, D. J. *J. Magn. Reson.* **1982**, *48*, 286.
(24) Lightfoot, P.; Woodcock, D. A.; Jorgensen, J. D.; Short, S. *Int. J. Inorg. Mater.* **1999**, *1*, *53*.

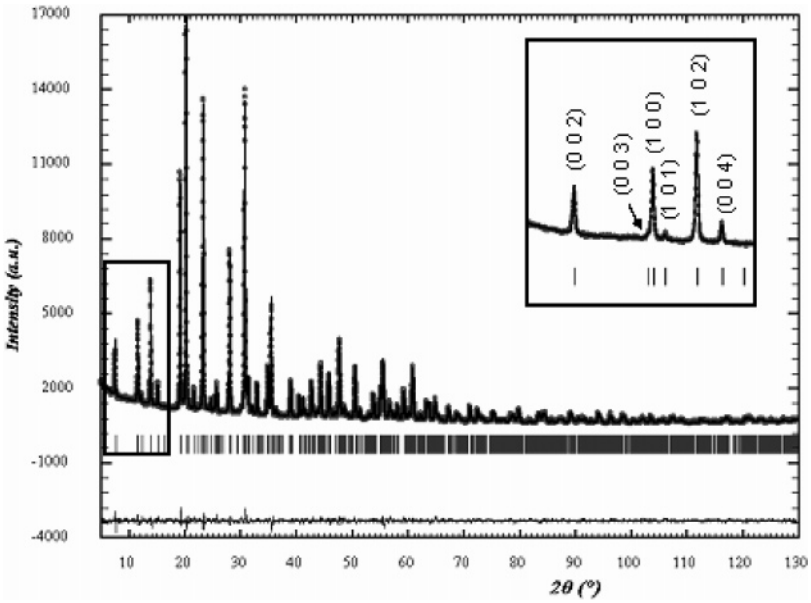

Figure 2. Observed and calculated powder X-ray diffraction patterns for $La_{1/3}Zr_2(PO_4)_3$ in the $P\bar{3}$ space group (No. 147). The difference pattern is shown below at the same scale (vertical bars are related to the calculated Bragg reflection positions).

Table 3. $La_{1/3}B_2(PO_4)_3$: $R\bar{3} \rightarrow P\bar{3}$ Transposition of Possible Atomic Positions from $La_{1/3}Ti_2(PO_4)_3$ to $La_{1/3}Zr_2(PO_4)_3$

atom type	$R\bar{3}$ (No. 148) $La_{1/3}Ti_2(PO_4)_3$	$P\bar{3}$ (No. 147) $La_{1/3}Zr_2(PO_4)_3$
La^{3+}	3a,[a] (0, 0, 0) 3b, (0, 0, $^1/_2$)	1a, (0, 0, 0) 1b, (0, 0, $^1/_2$) 2 × 2d, ($^1/_3$, $^2/_3$, *z*): $z = {}^2/_3$ and $^2/_3 + {}^1/_2$
B	2 × 6c, (0, 0, *z*): $z = 0.1469$ and 0.6424	2 × 2c, (0, 0, *z*): $z \approx 0.14$ and 0.65 4 × 2d ($^1/_3$, $^2/_3$, *z*) $z \approx 0.02$, 0.31, 0.53 and 0.80
P	18f, (*x*, *y*, *z*): 0.2854, 0.0047, 0.2517	3 × 6g, (*x*, *y*, *z*) 0.28, 0.99, 0.25 0.95, 0.33, 0.58 0.62, 0.66, 0.92
O	4 × 18f, (*x*, *y*, *z*): ...	12 × 6g, (*x*, *y*, *z*): ...

[a] La^{3+} ions are only located in this site (with a $^2/_3$ sof) for $La_{1/3}Ti_2(PO_4)_3$.[24]

Table 4. Results Structure Refinement of $La_{1/3}Zr_2(PO_4)_3$ [space group $P\bar{3}$ (No. 147) $Z = 6$; MW = 513.666 g/mol]

	X-ray	neutron
no. of refined parameters	118	95
peak shape, η	pseudo-Voigt 0.48(1)	pseudo-Voigt 0.86(1)
cell parameters (Å)	$a = 8.7492(2)$ $c = 23.2483(5)$	$a = 8.7378(2)$ $c = 23.2156(7)$
half-width parameters	$u = 0.052(4)$ $v = 0.012(3)$ $w = 0.0200(5)$ $x = 0.00509$	$u = 0.093(6)$ $v = -0.22(1)$ $w = 0.315(5)$ $x = -0.00519$
asymmetry parameters	$P_1 = 0.046(2)$ $P_2 = -0.0006(5)$	$P_1 = 0.021(3)$ $P_2 = 0.0056(9)$
R_{Bragg} (%)	3.07	3.66
R_p (%)	10.5	7.66
R_{wp} (%)	9.83	7.80
R_{exp} (%)	7.85	4.57
χ^2	1.57	2.91

the $R\bar{3}$ one for the analogous titanium compound.[24] Table 3 gathers the corresponding splitting of the possible atomic sites for the $La_{1/3}B_2(PO_4)_3$ (B = Ti or Zr). It can be seen that the number of adjustable parameters is then greatly increased: for the $[B_2(PO_4)_3]^-$ network, in the $R\bar{3}$ space group, 17 positional parameters (12 of which for the oxide ions), and 51 (36 of which for the oxide ions) for the $P\bar{3}$ space group. Under these conditions, it is easy to understand that a better and realistic convergence of the refinement calculations is reached by using soft-constrained P−O and Zr−O distances (here 1.52 and 2.10 Å respectively, with the same standard error, 0.01 Å) (Fullprof[14]). It is also to be noticed that, in the case of $Ca_{0.5}Zr_2(PO_4)_3$,[25] although crystallizing in the $R\bar{3}$ space group, it was claimed that the X-ray powder diffraction failed to provide accurate oxide ions coordinates. When the $[Zr_2(PO_4)_3]^-$ network refined atomic positions are judged stabilized, Fourier-difference calculations are performed and reveal four possible kinds of positions for the two La^{3+} ions of the unit cell; they correspond to the sites 1a (0, 0, 0) (La1), 1b (0, 0, $^1/_2$) (La2) and to two 2d sites ($^1/_3$, $^2/_3$, *z*) with $z \sim {}^2/_3$ (La3) and $^2/_3 + {}^1/_2$ (La4). All these sites corresponding to the M1 position type frequently described for NASICON structure in $R\bar{3}c$ space group.[24] Further refinements of their sof demonstrate that in fact the La4 site is empty and that the two La^{3+} ions of the unit cell are located as follows: 1 in the 1a site (La1), 0.82 in the 1b site (La2), and 0.18 in a 2d site (La3). This situation shows a quasiordering along the *c* axis of the two La^{3+} ions in the NASICON-type network, in contrast to the case of $La_{1/3}Ti_2(PO_4)_3$, where the two La^{3+} ions are found on the 3a site (0, 0, 0) of the $R\bar{3}$ space group. Figure 3 presents the projections of the structures of the $La_{1/3}Ti_2(PO_4)_3$ and $La_{1/3}Zr_2(PO_4)_3$ compounds. By another way, this ordering of La^{3+} ions along the *c* axis leads, normally in $La_{1/3}Zr_2(PO_4)_3$, to a strong decrease of the O10−O10 height (*d*) of the oxide antiprism surrounding the M1 position: 4.174 Å instead of 4.716 Å in the case of $La_{1/3}Ti_2(PO_4)_3$, where this site is empty. Table 4 gathers the refinement results and the *R* factors values, and Table 5 presents the final atomic parameters and B_{iso} values. Figure 2 presents the observed and calculated diffraction patterns.

(25) Alamo, J.; Rodrigo, J. L. *Solid State Ionics* **1999**, *63*−*65*. 678.

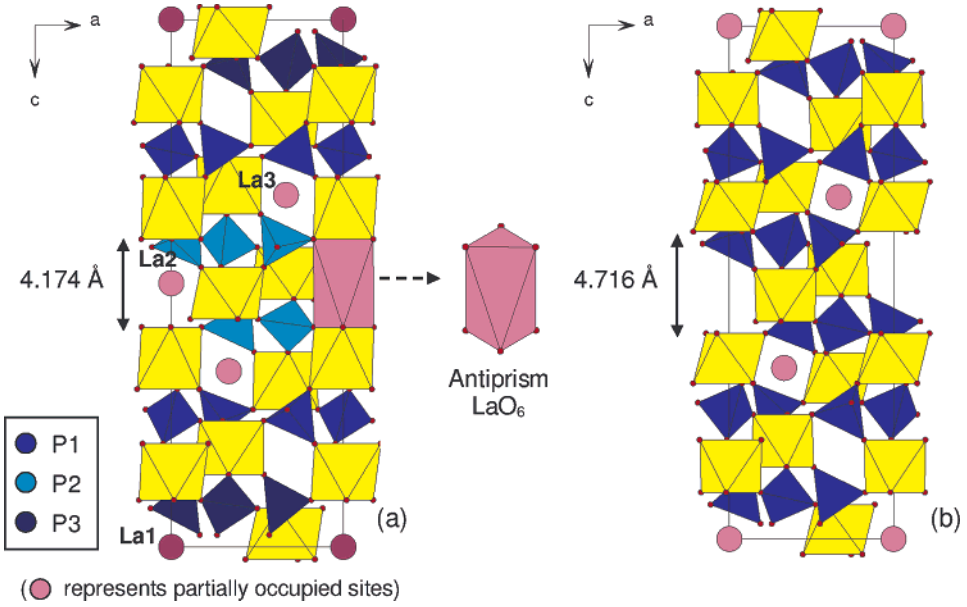

Figure 3. Projections of the structures of $La_{1/3}Zr_2(PO_4)_3$ (a) and $La_{1/3}Ti_2(PO_4)_3$ (b).

Table 5. Atomic Coordinates and B_{iso}[a] for $La_{1/3}Zr_2(PO_4)_3$

			x		*y*		*z*		*B* (10^{-2} Å^2)	
	site	sof	neutron	X-ray	neutron	X-ray	neutron	X-ray	neutron	X-ray
Zr1	2c	1	0	0	0	0	0.1501(9)	0.1513(3)	1.78(4)	0.34(3)
Zr2	2c	1	0	0	0	0	0.6526(9)	0.6514(3)	1.78(4)	0.34(3)
Zr3	2d	1	1/3	1/3	2/3	2/3	0.8104(9)	0.8123(4)	1.78(4)	0.34(3)
Zr4	2d	1	1/3	1/3	2/3	2/3	0.5241(9)	0.5258(4)	1.78(4)	0.34(3)
Zr5	2d	1	1/3	1/3	2/3	2/3	0.3131(9)	0.3123(4)	1.78(4)	0.34(3)
Zr6	2d	1	1/3	1/3	2/3	2/3	0.026(1)	0.0250(3)	1.78(4)	0.34(3)
P1	6g	1	0.2875(8)	0.2959(8)	0.002(1)	0.009(1)	0.2487(3)	0.2480(4)	1.82(4)	0.41(7)
P2	6g	1	0.9514(8)	0.948(1)	0.3186(9)	0.321(1)	0.5819(3)	0.5845(3)	1.82(4)	0.41(7)
P3	6g	1	0.6202(9)	0.6272(9)	0.6769(9)	0.6845(9)	0.9210(3)	0.9225(3)	1.82(4)	0.41(7)
O1	6g	1	0.1679(8)	0.146(2)	0.952(2)	0.927(2)	0.1957(5)	0.2042(7)	2.37(2)	0.03(9)
O2	6g	1	0.826(1)	0.824(3)	0.288(2)	0.307(4)	0.5309(4)	0.5363(7)	2.37(2)	0.03(9)
O3	6g	1	0.538(1)	0.537(2)	0.667(2)	0.699(3)	0.8627(3)	0.8677(7)	2.37(2)	0.03(9)
O4	6g	1	0.034(2)	0.024(4)	0.836(2)	0.806(2)	0.7006(5)	0.6952(6)	2.37(2)	0.03(9)
O5	6g	1	0.734(1)	0.742(3)	0.166(1)	0.178(3)	0.0234(3)	0.0234(8)	2.37(2)	0.03(9)
O6	6g	1	0.322(2)	0.350(4)	0.481(1)	0.473(3)	0.3690(4)	0.3587(7)	2.37(2)	0.03(9)
O7	6g	1	0.188(1)	0.187(2)	0.172(1)	0.165(3)	0.0890(6)	0.0909(7)	2.37(2)	0.03(9)
O8	6g	1	0.889(1)	0.906(2)	0.504(1)	0.495(2)	0.4312(6)	0.4345(8)	2.37(2)	0.03(9)
O9	6g	1	0.539(1)	0.521(2)	0.834(1)	0.833(3)	0.7606(6)	0.7516(6)	2.37(2)	0.03(9)
O10	6g	1	0.828(1)	0.815(3)	0.825(1)	0.820(2)	0.5838(5)	0.5938(8)	2.37(2)	0.03(9)
O11	6g	1	0.498(1)	0.495(2)	0.121(1)	0.116(2)	0.9266(6)	0.9251(8)	2.37(2)	0.03(9)
O12	6g	1	0.147(1)	0.145(3)	0.473(1)	0.470(2)	0.2603(5)	0.2602(8)	2.37(2)	0.03(9)
La1	1a	1	0	0	0	0	0	0	7.2(3)	5.5(1)
La2	1b	0.82(5)	0	0	0	0	1/2	1/2	7.2(3)	5.5(1)
La3	2d	0.09(3)	1/3	1/3	2/3	2/3	0.667(5)	0.669(5)	7.2(3)	5.5(1)

[a] To reduce the number of adjustable parameters, the refined B_{iso} are constrained at the same value for each kind of atom.

Neutron Diffraction Study. This study was undertaken in order to improve the precision of the atomic parameters of the light atoms (P and O). The refinement calculations led to a good convergence by using only a P−O soft-constrained distance (1.52 Å with a 0.01 Å standard error, the same values as for the XRD study). A Fourier-difference calculation and further refinements confirm the La^{3+} ions location found from the XRD data. Table 4 gathers the refinement results and the final values of the *R* factors, and Table 5 shows the final atomic coordinates and B_{iso} values, which are more realistic than those found from XRD refinement. The observed and calculated diffraction patterns are shown at Figure 4. The atomic coordinates obtained from the neutron diffraction data are those that we finally keep to describe the structure hereafter.

^{31}P NMR Results. In a first step, MAS one-dimensional (1D) one-pulse experiments were performed on ^{31}P nuclei.

The spectrum is shown in Figure 5 and its characteristic are given in Table 6. To account for the 1D spectrum, we need five lines that can be attributed to five phosphorus sites. The most intense contributions appear at −34.2 ppm [29%, P(1)], −23.3 ppm [29%, P(2)], and −22.5 ppm [33%, P(3)], and two other weak contributions appear at −31.6 ppm [3%, P(4)] and at −22.3 ppm [7%, P(5)]. The 2D data (Figure 6) provides evidence that P(1), P(2), and P(3) are autocorrelated [peaks (1−1), (2−2), and (3−3)]. P(1) is intercorrelated with P(2) and P(3), and P(2) and P(3) are not correlated. So P(1), P(2), and P(3) belong to the same homogeneous phase. The other phosphorus atoms P(4) and P(5) do not evidence any correlation with either P(1), P(2), P(3) or themselves. So we

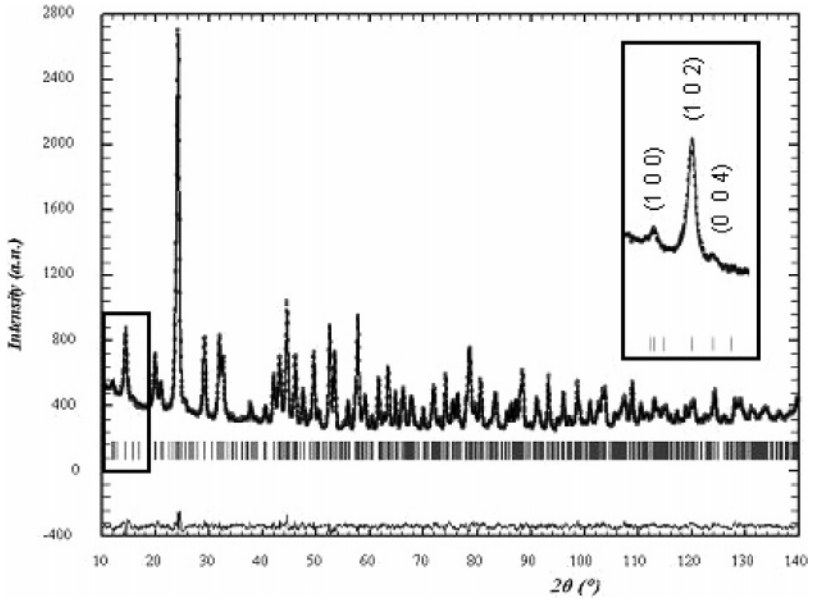

Figure 4. Observed and calculated powder neutron diffraction patterns for $La_{1/3}Zr_2(PO_4)_3$ in the $P\bar{3}$ space group (No. 147). The difference pattern is shown below at the same scale (vertical bars are related to the calculated Bragg reflection positions).

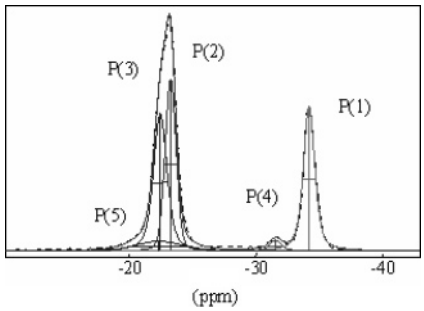

Figure 5. ^{31}P NMR MAS spectrum of $La_{1/3}Zr_2(PO_4)_3$: dotted points, experimental; solid line, calculated; fine line, different contributions.

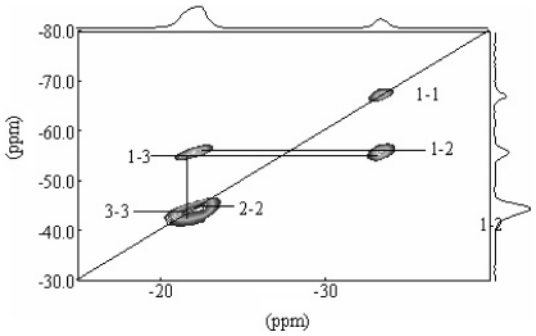

Figure 6. ^{31}P NMR DQ spectrum of $La_{1/3}Zr_2(PO_4)_3$.

Table 6. Analysis of the ^{31}P NMR MAS Spectrum of $La_{1/3}Zr_2(PO_4)_3$

line	T_1 (s)	δ_{iso} (ppm) ± 0.2	width (ppm) ± 0.1	% ± 1
P(1)	131	−34.2	1.1	29
P(2)	131	−23.3	1.0	29
P(3)	131	−22.5	1.3	33
P(4)	84	−31.6	1.2	3
P(5)		−22.3	4.4	7

Table 7. Selected Interatomic Distances (Å) in $La_{1/3}Zr_2(PO_4)_3$ (from neutron data refinement)

Zr octahedron	P tetrahedron	La polyhedron
Zr1−O1: 3 × 2.02(2)	P1−O1: 1.49(1)	La1−O7: 6 × 2.60(2)
Zr1−O7: 3 × 2.12(2)	P1−O4: 1.507(9)	
<*Zr1−O*>: 2.07	P1−O9: 1.53(2)	
Zr2−O4: 3 × 1.95(2)	P1−O12: 1.53(1)	
Zr2−O10:3 × 2.20(2)	<*P1−O*>: 1.51	
<*Zr2−O*>: 2.08		
Zr3−O9: 3 × 2.02(2)	P2−O2: 1.50(1)	La2−O10: 6 × 2.47(2)
Zr3−O3: 3 × 2.16(2)	P2−O6: 1.51(1)	
<*Zr3−O*>: 2.09	P2−O8: 1.52(1)	
Zr4−O8: 3 × 2.04(2)	P2−O10: 1.54(1)	
Zr4−O2: 3 × 2.07(2)	<*P2−O*>: 1.52	
<*Zr4−O*>: 2.05		
Zr5−O6: 3 × 2.04(2)	P3−O3: 1.52(1)	La3−O9: 3 × 2.7(2)
Zr5−O12: 3 × 2.06(2)	P3−O5: 1.53(1)	La3−O8: 3 × 2.9(2)
<*Zr5−O*>: 2.05	P3−O7: 1.55(1)	<*La3−O*>: 2.8
Zr6−O5: 3 × 2.02(2)	P3−O11: 1.55(1)	
Zr6−O11: 3 × 2.16(2)	<*P3−O*>: 1.54	
<*Zr6−O*>: 2.09		

think that P(4) and P(5) belong to other domains. This behavior could correspond to the contributions arising from the phosphorus near the few lanthanum ions located on site 2d (La3). We can consider that the three contributions P(1), P(2), and P(3) have to be attributed to the crystallographic 6g sites: P1, P2, P3 (Table 5). By considering the positions of the lines (in which the most screened nucleus appear in the high side of spectrum), we can attribute P(1) to P1 with no La^{3+} as second neighbor and P(2) and P(3) both to phosphorus in the P2 and P3 sites.

Discussion

As expected, the $[Zr_2(PO_4)_3]^-$ network, encountered in other NASICON-type compounds exhibiting higher symmetry, is preserved here and presents conventional interatomic distances and valence sums, as can be seen in Tables 7 and 8, respectively. By contrast, the La^{3+} ions—all in a 6-fold coordination—exhibit a high B_{iso} value [7.2(3) and 5.5(1) Å from neutron and X-ray data, respectively] associated to quite large La−O distances (6 × 2.60 Å for La1−O7, 6 × 2.47 Å for La2−O10, and 3 × 2.70 Å and 3 × 2.90 Å for La3−O9 and La3−O8, respectively) in comparison with the sum of the ionic radii (2.38 Å corresponding to 1.032 Å + 1.35 Å, the radii of La^{3+} and O^{2-} in a 6-fold and a 2-fold coordination, respectively[27]). This fact leads consequently

(26) Brese, N. E.; O'Keeffe, M. *Acta Crystallogr.* **1991**, *B47*, 192.

Table 8. Bond Valence Analysis for $La_{1/3}Zr_2(PO_4)_3$ Using the Zachariasen Law[26]

atoms	O1	O2	O3	O4	O5	O6	O7	O8	O9	O10	O11	O12	Σ	Σ_{exp}
Zr1	3 × 0.80						3 × 0.61						4.23	4
Zr2				3 × 0.96						3 × 0.48			4.32	4
Zr3			3 × 0.80						3 × 0.55				4.05	4
Zr4		3 × 0.75						3 × 0.70					4.35	4
Zr5						3 × 0.75						3 × 0.71	4.38	4
Zr6					3 × 0.80						3 × 0.55		4.05	4
P1	1.21			1.23					1.30			1.35	5.09	5
P2		1.18				1.31		1.28		1.26			5.03	5
P3			1.27		1.21		1.16				1.17		4.81	5
La1							6 × 0.32						1.92	3
La2										6 × 0.45			2.70	3
La3								3 × 0.15	3 × 0.22				1.11	3
Σ	2.01	1.93	2.07	2.19	2.01	2.06	2.09	1.98	2.07	2.19	1.72	2.06		
Σ_{exp}	2	2	2	2	2	2	2	2	2	2	2	2		

to low valence sums for La^{3+} (1.90, 2.70, and 1.11 for La1, La2, and La3, respectively, as shown at Table 8). A similar situation is observed for La^{3+} ions in $La_{1/3}Ti_2(PO_4)_3$ (only one site, 3a, with a $^2/_3$ sof in the $R\bar{3}$ space group)[24] where, on the basis of the published neutron powder diffraction results, we calculate a 2.33 valence sum for La^{3+} (corresponding to six equal 2.52 Å La−O distances). It is to be noticed that a valence sum equal to 3 for a La^{3+} ion in a regular 6-fold oxide coordination corresponds to a 2.428 Å La−O distance. We can conclude that, in these NASICON type compounds, the cages of their $[Zr_2(PO_4)_3]^-$ networks could accommodate cations with a larger radius than that of La^{3+}. This structural fact is in good agreement with the RE^{3+} ionic conductivity observed on these compounds.[5−11]

The NMR study (^{31}P MAS and 2D DQ experiments) allows us to determine the nature of the disordered average structural view brought by the X-ray and neutron diffraction experiments; it reveals that the sample is in fact constituted by two kinds of domains: one corresponding to the perfect ordering of the La^{3+} ions on the La1 and La2 positions (1a and 1b sites in the $P\bar{3}$ space group) and the other, with a very small size owing to the lack of autocorrelation, presenting some extra La^{3+} ions distributed on the La3 position (2d site in the $P\bar{3}$ space group).

Conclusion

$La_{1/3}Zr_2(PO_4)_3$ crystallizes at room temperature in $P\bar{3}$, a new space group in the NASICON materials family. It is demonstrated by X-ray and neutron powder diffraction and confirmed precisely by ^{31}P NMR experiments. The $[Zr_2(PO_4)_3]^-$ classical network is preserved and the major part of the La^{3+} ions preferentially occupies the sites 1a (0, 0, 0) and 1b (0, 0, $^1/_2$), the remaining being located dissymmetrically on one site 2d ($^1/_3$, $^2/_3$, z, with $z \approx {}^2/_3$). This situation of quasiperfect ordering of the two La^{3+} ions on the c axis of the unit cell, in one-third of the six usual M1 positions of the NASICON network, differs from that observed in the parent compound $La_{1/3}Ti_2(PO_4)_3$, where the two La^{3+} ions are distributed on the site 3a (0, 0, 0) of the $R\bar{3}$ space group.

Acknowledgment. We are indebted to the Institute Laüe-Langevin (ILL, Grenoble, France) for neutron beam-time allocation.

CM0515045

(27) Shannon, R. D. *Acta Crystallogr.* **1976**, *A32*, 751.